Reliability Engineering and System Safety 273 (2026) 112307

Contents lists available at ScienceDirect

Reliability Engineering and System Safety

journal homepage: www.elsevier.com/locate/ress

Nonlinear random walks on hypergraphs characterized by higher-order interactions

Meng Li [a], Xin Lu [b,*], Shuiling Shi [c,*], Leyang Xue [d], Zengru Di [e]

[a] School of Mathematics, Foshan University, 528000, Foshan, PR China
[b] College of Systems Engineering, National University of Defense Technology, 410073, Changsha, PR China
[c] Data Science Research Center, Kunming University of Science and Technology, 650500, Kunming, PR China
[d] Department of Physics, Bar-Ilan University, Ramat-Gan, 52900, Israel
[e] International Academic Center of Complex Systems, Beijing Normal University, 519087, Zhuhai, PR China

ARTICLE INFO

Keywords:
Hypergraphs
Higher-order interactions
Nonlinearity
Random walks

ABSTRACT

Random walks, as one of the classical dynamics on networks, are capable of extracting information on the structure of interacting systems. While existing studies have extended classical network random walks to higher-order networks, prevailing models primarily assume linear relationships between transition probabilities and node hyperdegrees or hyperedge sizes, which inadequately represent the nonlinear properties of higher-order interactions. To address this, we propose a nonlinear random walk on hypergraphs that explicitly considers higher-order collaborative structures and nonlinear dynamics. By introducing a nonlinear mapping between transition probabilities and node hyperdegrees, we go beyond the linear assumption constraints of traditional random walks. Specifically, the probability of a node selecting a hyperedge is inversely proportional to a power function of its hyperdegree, where the power exponent is determined by the interaction order. We first conduct qualitative analysis of the model on star-clique structures, comparing it with classical random walk and linear random walk to reveal the mechanism by which higher-order interactions influence node importance rankings. Subsequently, we conducted node removal experiments on three large-scale datasets to validate the effectiveness of the model by comparing three structural integrity metrics. The results indicate that the proposed model consistently outperforms both Classical and Linear models across all datasets and metrics. These findings confirm that accounting for the nonlinear characteristics of higher-order interactions is essential for both accurately identifying critical nodes and understanding system robustness.

1. Introduction

Complex systems are ubiquitous in nature and society, manifesting across diverse domains from biological ecosystems and neural networks to social organizations and technological infrastructures. These systems are characterized by numerous interconnected components that collectively exhibit emergent behaviors, self-organization, and adaptive capabilities that transcend the properties of individual constituents [1]. The intricate web of relationships within complex systems gives rise to non-trivial dynamics, including nonlinear responses to perturbations [2], critical transitions [3], and scale-invariant properties that cannot be explained by examining components in isolation [4,5].

In response to the analytical demands of complex systems, network science has emerged as a crucial methodology and ideal tool for exploring complexity through its capacity to structurally represent entity interactions—a mathematical framework that depicts entities as nodes and their relationships as edges [6–9]. Previous research has revealed that many interacting systems with vastly different functions exhibit remarkably similar structural properties across different scales [10]. From biological networks and brain connectomes to social networks and transportation systems, universal organizing principles such as small-world properties, scale-free degree distributions, and modular architectures continually emerge. These structural characteristics significantly influence the dynamical processes occurring on networks [11], including information diffusion, epidemic spreading, synchronization, and random walks. However, traditional network models are fundamentally limited to pairwise interactions, capable of encoding only pairwise interactions [12]. In many real-world systems, interactions between entities are not confined to relationships between pairs of nodes, but rather manifest as higher-order cooperative interactions among multiple groups (≥ 3) [13]. For example, synchronized firing of neuronal clusters requires multi-cellular electrical signal resonance to achieve cognitive functional

* Corresponding authors.
E-mail addresses: xin.lu.lab@outlook.com (X. Lu), shishuiling0409@sina.com (S. Shi).

https://doi.org/10.1016/j.ress.2026.112307

Available online 31 January 2026

transitions [14]; cascade outbreaks of public opinion in social systems are often triggered by three or more core users [15]; and gene regulation in biological systems depends on the synergistic action of multiple transcription factor complexes [16]. Similarly, power distribution networks rely on the synchronized operation of multiple substations and switching nodes, where voltage stability can be maintained through collective coordination rather than individual node performance [17]. Distributed computing systems require coordinated processing across multiple server nodes for data partitioning, parallel computation, and result aggregation [18]. In these infrastructure systems, the failure or disruption of components can trigger cascading effects that propagate through higher-order dependencies, making traditional pairwise models insufficient for reliability assessment and risk management [19,20]. These higher-order interaction effects cannot be achieved through simple aggregation of pairwise relationships and require mathematical tools such as hypergraphs or simplicial complexes to construct higher-order networks for their representation.

The mathematical frameworks of hypergraphs and simplicial complexes have enabled researchers to formalize higher-order interactions and develop analytical tools for studying the resulting dynamics [21–23]. While simplicial complexes enforce hierarchical inclusion of lower-dimensional simplices, hypergraphs offer greater flexibility by allowing arbitrary group formations, making them particularly suitable for systems where higher-order interactions need not contain all subgroup interactions. These mathematical structures provide the foundation for modeling complex systems where interactions occur among multiple entities simultaneously, moving beyond the limitations of traditional graph-based representations.

The recognition of higher-order interactions has fundamentally transformed our understanding of dynamical processes on complex systems. Recent studies have demonstrated that incorporating higher-order interactions leads to qualitatively different behaviors across various dynamical processes compared to traditional network models limited to pairwise interactions [24]. These emergent phenomena include abrupt phase transitions in spreading processes [25], enhanced synchronization stability [26,27], and novel pattern formation in reaction-diffusion systems [28]. Furthermore, recent research has revealed that the spectral properties of higher-order Laplacian operators, which govern numerous dynamical processes, exhibit fundamentally different characteristics compared to their graph counterparts [29]. These differences manifest in altered diffusion patterns, modified community structures, and distinctive centrality measures.

It is noteworthy that among the various dynamical processes studied on higher-order structures, random walks represent a fundamental dynamical process with far-reaching applications across diverse fields, providing profound insights into diffusion processes, community detection, and centrality measures in complex systems. However, existing random walk models typically assume pairwise interactions and linear dynamics, failing to capture the complexity of many real-world systems. This recognition necessitates the development of more sophisticated mathematical frameworks. In this paper, we investigate higher-order group interactions using hypergraph representations, with a particular focus on their nonlinear dynamical properties. We introduce a nonlinear function to establish the mapping between transition probabilities and node hyperdegrees, overcoming through the linear assumption constraints inherent in traditional random walks, and develop a nonlinear random walk model on hypergraphs that captures higher-order interaction effects.

The remainder of this paper is organized as follows. Section 2 provides an overview of related literature. In Section 3, we propose a nonlinear random walk model on hypergraphs with high-order interactions, and analyze the convergence of the model. In Section 4, we conduct extensive simulation experiments to explore the fundamental properties of the proposed random walk model in high-order structures, thereby gaining deeper insights into the qualitative behavior of the model. We also perform comprehensive experimental validation to evaluate the performance of the model in critical node identification. Finally, Section 5 concludes the paper and briefly discusses future research directions.

2. Related work

This section reviews the literature on higher-order network dynamics, with a particular focus on the research progress and applications of propagation dynamics and random walk models based on hypergraphs.

2.1. Dynamics on higher-order networks

Recent years witness growing interest in the dynamics of complex systems with higher-order interactions. In higher-order networks represented by hypergraphs or simplicial complexes, collective interactions among groups of nodes can fundamentally alter system dynamics. Battiston et al. [30] provide a comprehensive review of this emerging field, highlighting the fundamental differences between dynamics on these structures compared to traditional network processes.

In epidemic modeling, Bodó et al. [31] introduce a generalized SIS model based on hypergraphs, in which an infection occurs if sufficiently many infected individuals coexist within a hyperedge. This formulation reveals that the epidemic threshold is influenced by hyperedge size and internal composition, with nonlinear infection dynamics arising from higher-order exposure. Building on this framework, researchers extend this approach to simplicial complexes, considering infections occurring in triangles and higher-dimensional simplices [15]. Their findings demonstrate that continuous and discontinuous phase transitions emerge depending on the order and strength of group interactions—phenomena intrinsically absent in binary networks.

To explore the role of temporal and adaptive higher-order structures, researchers [32] investigate contagion processes on time-varying hypergraphs, showing that the formation and dissolution of dynamic hyperedges significantly impact spreading efficiency and critical thresholds. Subsequent work by Arruda et al. [33] incorporates memory and reinforcement mechanisms into higher-order contagion, demonstrating that repeated contacts within small groups substantially alter contagion dynamics and may trigger abrupt transitions.

Recent studies introduce nonlinear threshold mechanisms on hypergraphs. The contagion model proposed in reference[34] incorporates group influence within hyperedges and shows that higher-order exposure can induce rich dynamical patterns, including multistability, intermittency, and mixed-phase transitions. The authors note that both hyperedge size and adoption thresholds significantly affect the macroscopic behavior of system, further highlighting the critical role of higher-order topology in determining the collective dynamics of social influence. Furthermore, other dynamical processes, such as consensus formation [35,36] and synchronization [37], are also generalized to higher-order frameworks.

2.2. Random walks on hypergraphs

Random walks represent a fundamental class of dynamical processes on complex networks. On classical networks, random walks can be divided into two steps: i) At each time step, the random walker at the current node randomly selects an available edge with uniform probability; ii) The walker jumps to one of its adjacent nodes through this edge. Based on the classical model, scholars have considered many variants[38,39]. Similarly, random walks can be defined on higher-order networks. In simplicial complexes, Schaub et al. proposed random walks by generalizing the relationship between graph Laplacians and random walks on graphs, where random walkers occupy edges rather than nodes[40]. In addition, researchers considered special cases of simplicial complexes where each edge is included in at most two 2-simplices, proposing another type of random walk on simplicial complexes[41]. According to their formulation, at each time step, a random walker at a

2-simplex remains stationary with probability 1/2, or transitions to one of the three edges with probability 1/6 each.

Unlike simplicial complexes, hypergraphs can represent interactions of any order, allowing for more general random walk formulations. Zhou et al. [42] proposed a random walk model on weighted hypergraphs, where the random walker first selects a hyperedge from all hyperedges containing the current node with probability proportional to the hyperedge weight, then uniformly selects a node within that hyperedge. We refer to this approach as the Classical Random Walk (CRW) throughout this paper. Carletti et al. [43] developed a linear random walk framework for hypergraphs. In their model, the transition probability from node i to node j is linearly proportional to the total size of all hyperedges containing both nodes. This mechanism naturally leads to random walkers spending extended periods within larger hyperedges, as these structures are selected with higher probability during the transition process. This approach is denoted as the Linear Random Walk (LRW) in our subsequent analysis.

Several researchers have investigated the properties of random walks on random hypergraphs [44], particularly in the case of a unique giant component. Through spectral decomposition methods, they analyzed the asymptotic behavior of hitting times, commute times, and cover times, demonstrating that these results exhibit universality comparable to random walks on random graphs. Furthermore, beyond assigning weights to hyperedges, node weights can also be considered [45], where nodes within the same hyperedge are allocated different weights. In this weighted framework, the probability of a random walker selecting a hyperedge is the ratio of the hyperedge weight to the degree of the current node, and the probability of selecting a node is the ratio of the node weight to the degree of the hyperedge. Recently, Lú et al. [46] introduced a multi-order graph obtained by incorporating the higher-order bipartite graph and the classical pairwise graph, thereby preserving both binary relationships and high-order interaction information between nodes in the same model, and designed a Higher-order augmented random walk model through random walking on the proposed multi-order graph.

Although existing random walks on hypergraphs have provided valuable analytical frameworks for higher-order networks, these approaches are typically based on linear assumptions, presuming that the transition probabilities exhibit a linear relationship with the node's hyperdegree or the weights of hyperedges. This assumption fails to adequately capture the complexity of higher-order interactions involving multiple entities, potentially leading to an inaccurate representation of the dynamics of real systems. This paper constructs a nonlinear random walk on hypergraphs with higher-order interactions, providing a novel tool for complex systems modeling and helping to reveal the influence of higher-order interactions on nodes ranking in higher-order networks.

3. Methods

3.1. Definition of a hypergraph

Hypergraph structures can represent fundamentally different scenarios. In some cases, the specific set of entities is semantically meaningful. For instance, a research paper represents a collaboration among a specific group of authors, where adding or removing any author creates a fundamentally different entity. In other cases, hypergraphs simply serve as a structural formalism to aggregate pairwise interactions. To distinguish these different interpretations, it is necessary to precisely define higher-order interactions. An interaction is defined as a set $I = \{p_0, p_1, \cdots, p_{k-1}\}$ containing any k basic elements in the system, which are called nodes. Such interactions can describe different scenarios in real systems, such as co-authors of scientific papers, a set of genes required to perform a certain function, and so forth. The order of an interaction involving k nodes is defined as $k-1$, where a node interacting only with itself represents a 0−order interaction, interaction between two nodes is 1-order, interaction among three nodes is 2-order, and so on. Furthermore, k-interactions with $k \geq 2$ are higher-order interactions, while interactions with $k \leq 1$ are lower-order interactions. Therefore, lower-order systems are those occurring in self or pairwise interactions, whereas higher-order systems represent systems composed of group interactions involving more than two elements.

Let us consider a hypergraph $H(V, E)$, where $V = \{v_1, v_2, \cdots, v_n\}$ and $E = \{E_1, E_2, \cdots, E_m\}$ represent the nodes set and the hyperedges set respectively, such that for any $\alpha = 1, 2, \cdots, m$, we have $E_\alpha \subset V$. Then, the elements $c_{i\alpha}$ of the incidence matrix $C_{n\times m}$ can be expressed as

$$c_{i\alpha} = \begin{cases} 1, & if\ v_i \in E_\alpha, \\ 0, & otherwise. \end{cases} \tag{1}$$

This matrix describes the information shared between nodes on hyperedges. The adjacency matrix A can be represented by the incidence matrix as $A_{ij} = CC^T - D$, where A_{ij} indicates the number of hyperedges that contain both nodes v_i and v_j, D is a diagonal matrix, and C^T is the transpose of the incidence matrix C. D_{ii} represents the number of hyperedges to which node v_i belongs, which is the hyperdegree of the node. For notational convenience, we denote the hyperdegree of node v_i as $d_i = \sum_\alpha c_{i\alpha}$ in the subsequent discussion. The hyperedge matrix is defined as $K_{\alpha\beta} = C^T C$, where $k_{\alpha\beta}$ counts the number of nodes in $E_\alpha \cap E_\beta$. The number of nodes in hyperedge E_α is called the hyperedge degree, also known as the size of the hyperedge, denoted as $|E_\alpha| = \sum_{v\in V} c_{i\alpha}$. Fig. 1(a) provides an example containing 6 nodes and 3 hyperedges, with the corresponding incidence matrix C, adjacency matrix A, and hyperedge matrix K shown in Figs. 1(b), 1(c), and 1(d), respectively.

3.2. Nonlinear random walks on hypergraphs

The key to random walks lies in defining the transition probability from the current node to the next node at each time step. In classical random walks on hypergraphs, the walker selects any adjacent node with uniform probability. However, this simplified model fails to adequately capture the complex higher-order interactions among multiple entities in real-world systems. In fact, nodes belonging to the same hyperedge exhibit specific collaborative relationships, and as the order of interaction increases, the complexity of achieving effective collaboration grows nonlinearly. Taking scientific collaboration networks as an example, a paper co-authored by multiple researchers can be represented as a hyperedge, with each author constituting a node. Hyperedges of different orders represent different collaboration patterns, and the higher the order, the more complex the coordination mechanisms required, which cannot be simply regarded as a linear combination of lower-order interactions. In the framework of random walks with higher-order interactions, adding nodes not only alters the structure of the hypergraph but also requires consideration of the higher-order interaction effects brought by the nodes. This makes the interactions between nodes more complex and directly affects the calculation of transition probabilities. This structural change means that an increase in nodes will lead to more complex dynamic behaviors, influencing the movement paths of the walker within the hypergraph. Therefore, hyperedges and their constituent nodes have clear physical meanings, reflecting the complex collaborative mechanisms in real systems, which cannot be accurately described by simple uniform probability models.

We introduce a novel hypergraph random walk framework that explicitly accounts for the varying interaction complexity represented by hyperedges of different sizes. The walker's transition mechanism consists of two phases: first, selecting a hyperedge based on a hyperdegree-dependent nonlinear probability distribution, then uniformly choosing a node within the selected hyperedge. Specifically, the probability of the current node selecting a hyperedge is inversely proportional to a power function of its hyperdegree, where the power exponent equals the interaction order (i.e., the number of nodes in the hyperedge minus one). This formulation naturally captures the nonlinearly increasing coordination difficulty as group size grows, reflecting the essential characteristics of complex collaborative relationships in real-world scenarios. We

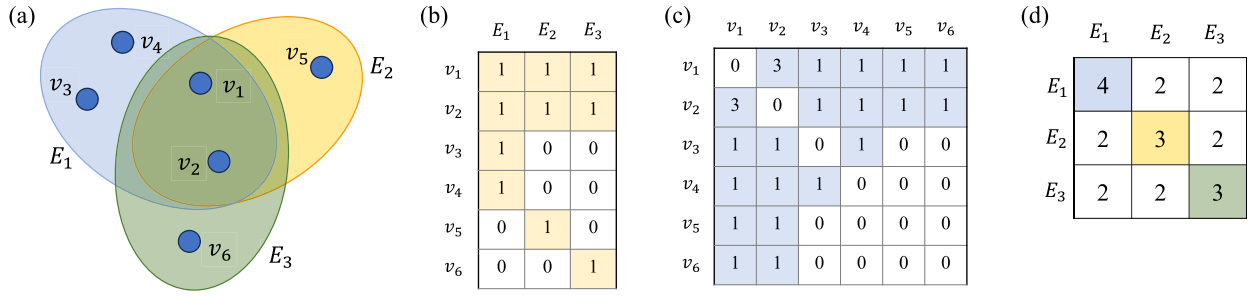

Fig. 1. (a) A hypergraph with 6 nodes and 3 hyperedges; (b)-(d) are the incidence matrix, adjacency matrix and hyperedge matrix of (a), respectively.

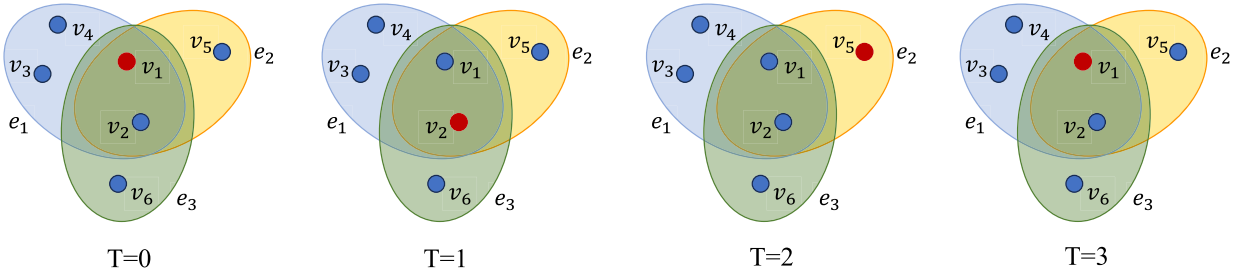

Fig. 2. Schematic diagram of the random walk process, the red node represents the node occupied by the walker.

refer to our proposed approach as the Nonlinear Random Walk (NRW). Formally, the probability for node v_i to select hyperedge E_α is

$$p_{i\alpha} = \frac{d_i^{-(|E_\alpha|-1)}}{\sum_{\beta: i\in E_\beta} d_i^{-(|E_\beta|-1)}}. \tag{2}$$

Here, d_i represents the hyperdegree of node v_i, and $|E_\alpha|-1$ reflects the order of interaction. The higher the order of interaction, the smaller the probability of selecting the hyperedge. The denominator is used for normalization, ensuring a uniform selection among the connected hyperedges. After selecting the hyperedge E_α, the walker transfers to a node within the hyperedge with a uniform probability of $1/|E_\alpha|$. Therefore, we can deduce the transition probability as

$$T_{ij} = \sum_{\alpha: i,j\in\alpha} p_{i\alpha}\cdot\frac{1}{|E_\alpha|} = \frac{d_i^{-(|E_\alpha|-1)}}{\sum_{\beta: i\in E_\beta} d_i^{-(|E_\beta|-1)}}\cdot\frac{1}{|E_\alpha|}. \tag{3}$$

At each time step, the walker selects a node to jump to based on the transition probabilities. As shown in Fig. 2.

When all hyperedges in the hypergraph contain exactly two different nodes, that is, $|E_\alpha| = 2$ for any $\alpha = 1, 2, \cdots, m$, the hypergraph appears to degenerate into a network with each hyperedge corresponding to an edge. In this case, the transition probability simplifies to

$$T^{(1)}_{ij} = \sum_{\alpha: i,j\in E_\alpha} \frac{d_i^{-1}}{\sum_{\beta: i\in E_\beta} d_i^{-1}}\cdot\frac{1}{2} = \frac{A_{ij}}{2d_i}, i\neq j. \tag{4}$$

This differs from the Classical Random Walk transition probability $T^{classical}_{ij} = \frac{A_{ij}}{k_i}$ by a factor of $\frac{1}{2}$, here k_i represents the degree of node v_i in the network. The essential difference is that although each hyperedge contains only two nodes, the hypergraph structure remains fundamentally distinct from networks because hyperedges naturally allow self-transitions. In a hyperedge $E_\alpha = \{v_i, v_j\}$, node v_i can transition to itself with probability $\frac{1}{2}$, while networks generally do not contain self-loops.

3.3. Existence of stationary distribution

Having established the transition probabilities for hypergraph random walks, we proceed to investigate the temporal evolution behavior of the random walk. We prove the existence of a stationary distribution for the proposed hypergraph random walk.

Assuming the hypergraph H is connected, the random walk possesses a steady-state distribution. To demonstrate this, we first formulate the dynamical equation that governs the temporal evolution of the probability vector $\mathbf{p}(t) = (p_1(t), p_2(t), \ldots, p_n(t))$, where $p_i(t)$ represents the probability of finding the walker at node i after t steps. The evolution of this probability distribution is governed by the equation

$$\mathbf{p}(t+1) = \mathbf{p}(t)T, \tag{5}$$

where T is the transition matrix with elements T_{ij}, and the equation corresponds to a Markov chain. For a connected hypergraph H, the random walk defined by the transition matrix T converges to a unique steady-state distribution $\boldsymbol{\pi}$ that satisfies $\boldsymbol{\pi} = \boldsymbol{\pi}T$. To establish this convergence, we need to show that the corresponding Markov chain is irreducible and aperiodic.

Since the hypergraph H is connected, for any pair of nodes i and j, there exists a sequence of hyperedges that connects them. Specifically, there exists a path of hyperedges $E_{\alpha_1}, E_{\alpha_2}, \ldots, E_{\alpha_k}$ such that $i\in E_{\alpha_1}$, $j\in E_{\alpha_k}$, and $E_{\alpha_l}\cap E_{\alpha_{l+1}}\neq\emptyset$ for $l = 1, 2, \ldots, k-1$. For each consecutive pair of hyperedges sharing at least one common node, the walker can transition from any node in one hyperedge to any other node in the same hyperedge with positive probability, and then move to the adjacent hyperedge through the shared node. This establishes that there exists a finite number of steps t such that $(T^t)_{ij} > 0$ for all pairs (i, j), proving irreducibility.

For aperiodicity, consider any hyperedge E_α with $|E_\alpha|\geq 3$. For any node $i\in E_\alpha$, the walker can perform a two-step return $v_i\to v_j\to v_i$ within this hyperedge, which yields $(T^2)_{ii} > 0$. Under structural diversity conditions typically satisfied by real-world hypergraphs, different return path lengths can be constructed, such that the greatest common divisor of $m: (T^m)_{ii} > 0$ equals 1, establishing aperiodicity (detailed proof in Supplementary Materials).

By the Perron-Frobenius theorem, an irreducible and aperiodic stochastic matrix admits a unique stationary distribution.

4. Experiments

The stationary visitation probability of random walks serves as a crucial metric for characterizing node centrality in networks, reflecting the long-term probability distribution of a walker's visits to each node obtained from numerical simulations. Ranking nodes according to this probability distribution can effectively identify important nodes within the network: the higher the probability of a walker visits a particular node, the greater its importance or centrality in the network. This centrality measure based on random walks has been extensively applied across various domains of network analysis, including web page ranking, social network influence analysis, and identification of key proteins in biological networks. However, the presence of higher-order interactions can significantly alter the importance ranking of nodes. In hypergraph structures, the scale and heterogeneity of hyperedges influence the transition probability distribution of random walks, thereby modifying the stationary distribution. This makes traditional centrality measures based on pairwise connections potentially inadequate for accurately reflecting the true status of nodes in higher-order networks.

4.1. Toy example analysis

This section systematically analyzes the changing patterns of random walk stationary distributions across different hypergraph structures, and explores how higher-order interactions reshape the importance ranking of nodes in networks. To demonstrate the impact of higher-order interactions in our proposed random walk model on hypergraphs, we consider a hypergraph with a specific structure. This hypergraph consists of m hyperedges of size 3, all of which share a common node that we refer to as the hub node (denoted as h). Additionally, there is one node that belongs to both one of the 3-hyperedge and a larger hyperedge of size k (forming a clique structure). We term this node as the clique node (represented as c), as illustrated in Fig. 3(a) for the case where $m = 4$ and $k = 6$.

After establishing the structural characteristics of the hypergraph, this study aims to validate that the proposed nonlinear random walk can effectively reveal higher-order interactions in groups by examining how it alters node importance rankings. To this end, we compare the stationary probabilities $p_i^{(\infty)}$ of three random walk approaches, and the corresponding results are presented on the left side of panel (c).

Classical Random Walk is essentially performed on the projected network, ranking nodes according to their degrees. Given that all m hyperedges are of size 3, with the hub node v_0 contributing a degree of 2 in each hyperedge. When $m > \frac{k}{2}$, the hub node v_0 achieves a total degree of $k_0 = 2m$, ranking first, followed by the clique node v_8 and other nodes. In the Linear Random Walk, the transition probability between two nodes is proportional to the total number of nodes contained in the hyperedges they share. This linear weighting scheme overemphasizes local density. As shown in panel (c) (orange bars), the c node achieves the highest stationary probability, followed by clique nodes with approximately equal probabilities. While the h node ranks only third despite its bridging role. Nodes in the m hyperedges show the lowest probabilities. This demonstrates that the linear model rewards local density over global structural importance.

In our Nonlinear Random Walk, high-order interactions within large hyperedges present nonlinear resistance to random walkers. In panel (c) (blue bars), the h node maintains the highest stationary probability $p_i^{(\infty)}$, correctly reflecting its global bridging role, followed by the c node. However, the $p_i^{(\infty)}$ of other nodes exhibit a pattern opposite to that of the linear method, the $p_i^{(\infty)}$ values of nodes within the m hyperedges are significantly higher than those of clique nodes. This ranking pattern demonstrates that the proposed model not only reflects how higher-order interactions reshape node importance, but also captures the global structural roles of nodes across the hypergraph. Furthermore, calculating the theoretical solution is crucial for validating our numerical simulation results and providing a precise mathematical benchmark. The theoretical solution is equivalent to finding the left eigenvector corresponding to the eigenvalue of 1 for the transition probability matrix, which represents the theoretical stationary distribution of the Nonlinear Random Walk. In panel (c) of Fig. 3, we mark the theoretical solution of the Nonlinear Random Walk with solid red dots, and we can observe that the simulation values and theoretical values are in perfect agreement.

First hitting time represents a fundamental metric in random walk analysis, defined as the number of steps required to reach node v_j for the first time when starting from node v_i. Given the stochastic nature of random walks, the first hitting time between any pair of nodes varies across different realizations. Consequently, we computed the average first hitting time (FHT) to characterize this property, with our findings illustrated on the right side of panel (c). Interestingly, when comparing FHT across the three random walk models, we observe patterns that are opposite to their stationary distributions. In the Classical Random Walk, node h has the shortest FHT, followed by node c, and then other nodes. In the Linear Random Walk, node c has the shortest FHT, followed by the other nodes in the clique, then node h, and finally the remaining nodes in the m hyperedges. In our proposed Nonlinear Random Walk, however, the FHT differences are substantially more pronounced. Node h maintains an extremely short FHT, followed by node c, then the remaining nodes within the m hyperedges, while the remaining nodes in the clique exhibit exceptionally long FHTs. These findings clearly demonstrate how higher-order interactions influence information propagation efficiency—specifically, the higher the order, the greater the interaction resistance, resulting in significantly reduced accessibility among nodes within large hyperedges. This distinctive behavioral characteristic forms a stark contrast with the predictions of traditional random walk models, highlighting the unique advantages of our model in capturing higher-order network dynamics.

Finally, we compared how the stationary probabilities $p^{(\infty)}$ of nodes h and c depend on parameter m across the three random walk models. As m increases, $p_h^{(\infty)}$ consistently increases while $p_c^{(\infty)}$ decreases in all three models. Interestingly, at $m = 7$, we observe that $p_h^{(\infty)}$ nearly equals $p_c^{(\infty)}$ in the linear model. Although the linear random walk inherently favors nodes in larger hyperedges, node h compensates by participating in m small hyperedges simultaneously. As m increases, the cumulative contribution from these small hyperedges grows linearly. At $m = 7$, this cumulative weight becomes comparable to the contribution of node c from one small hyperedge plus the large clique, demonstrating that breadth of participation can offset the advantage of high-weight hyperedges in the linear model's additive structure.

4.2. Real-world experiments

To investigate the impact of higher-order interactions on random walk dynamics and validate the effectiveness of the proposed models, we construct hypergraphs from three empirical datasets spanning diverse domains. These experiments aim to demonstrate the advantages of our approach in identifying critical nodes. Below we provide detailed descriptions of these datasets.

4.2.1. Data description

We present three hypergraphs generated from real-world data across different research domains, which will be used in subsequent sections to validate the effectiveness of our proposed method. Table 1 provides the topological properties of these hypergraphs, as well as the meanings of nodes and hyperedges.

Scientist Collaboration Dataset. Scientific collaboration networks represent a natural application for hypergraph modeling. We use a publication dataset from the American Physical Society (APS) journals, comprising 482,566 papers and 236,883 authors. Since some papers in the

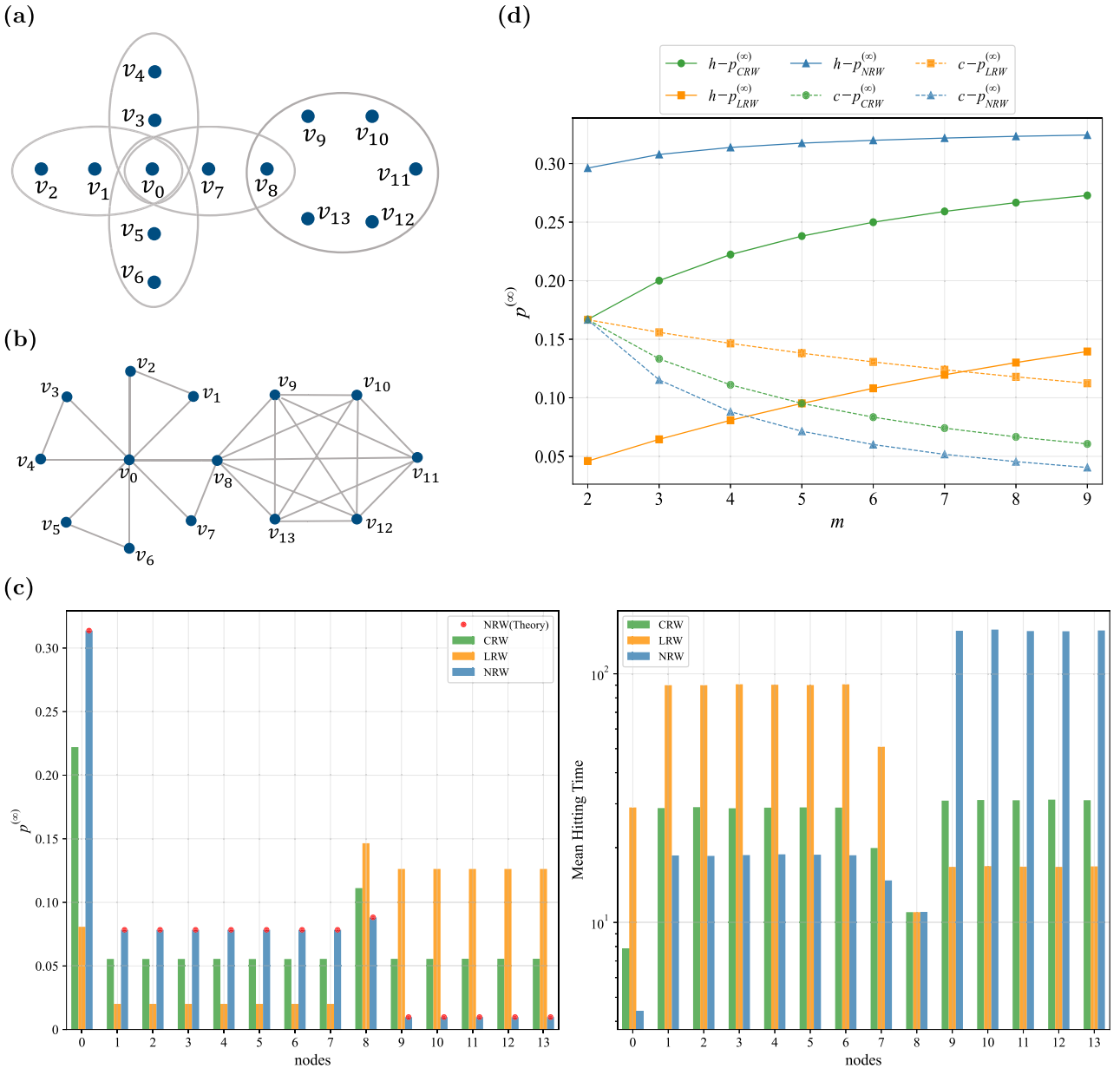

Fig. 3. An example of a star-clique structured hypergraph. (a) Hypergraph consisting of 5 hyperedges and 14 nodes, where the hub node v_0 has a hyperdegree of 4 with each hyperedge of size 3, and there is one large hyperedge of size 6. (b) The projected network of panel (a), where hyperedges are mapped to complete graphs, resulting in four 3-complete graphs on the left and one 6-complete graph on the right, connected by the c node v_8. (c) When $m = 4$ and $k = 6$, corresponding to panel (a), we compare the stationary distributions and first hitting times of Classical Random Walk, Linear Random Walk, and our proposed Nonlinear Random Walk. In the stationary distribution on the left side of panel (c), we mark the theoretical solution of the nonlinear random walk stationary distribution with solid red dots, and the first hitting times on the right is expressed in logarithmic scale. (d) Comparison of the stationary distributions of the three random walks for hub node h and clique node c depending on m. The results are averaged over 100 independent realizations.

dataset involve hundreds of authors—typically indicating large-scale collaborative projects that may introduce noise into the experimental results—we filter the dataset to retain only papers with at most 50 authors for constructing the scientific collaboration hypergraph. In this hypergraph, each paper corresponds to a hyperedge and each author to a node, yielding a final hypergraph with 228,008 nodes and 278,094 hyperedges.

Enron Email Dataset. The Enron Email dataset originated from the U.S. Federal Energy Regulatory Commission (FERC) investigation into the Enron corporate fraud case [35]. The constructed hypergraph contains 149 nodes representing key employees and 1452 hyperedges representing group Email communications. Each hyperedge connects one sender with multiple recipients in the same Email thread, excluding self-loop emails.

Geometry Dataset. The Geometry dataset is collected from MathOverflow.net, a question-and-answer platform for mathematics researchers. The constructed hypergraph contains 580 nodes representing users and 1193 hyperedges representing geometry-related questions. Each hyperedge connects a group of users who provided answers to the same geometry question.

Table 1
Summary of hypergraphs generated by three real-world datasets. The number of nodes N, the number of hyperedges M, the average degree $\langle k \rangle$, the average hyperdegree $\langle k^H \rangle$, and the average cardinality of hyperedges $\langle k^E \rangle$. The meanings of node and hyperedge in the metadata are presented in Node and Hyperedge.

Dataset	N	M	$\langle k \rangle$	$\langle k^H \rangle$	$\langle k^E \rangle$	Node	Hyperedge
APS	228,008	278,094	12.88	4.68	3.84	Author	Paper
Email-Enron	149	1452	25.16	31.32	3.08	Employee	Email
Geometry	580	1193	164.79	19.90	13.00	User	Question

Table 2
Comparison of Mean Rank and AUC of Nobel Prize laureates in Physics across three random walk models.

Method	Classical random walk	Linear random walk	**Nonlinear random walk**
Mean rank	29,268	51,980	**25234**
AUC	0.8719	0.7722	**0.8896**

4.2.2. Experimental results

We first conduct experiments on the APS dataset. Due to the large scale of this dataset, we perform 108 steps of random walks in each experiment to reduce the impact of random fluctuations. The academic influence of each author is determined by averaging the results of 50 independent experiments, which allows us to establish a ranking for each author. An effective model should assign higher rankings to more influential scientists. This dataset provides a natural benchmark for evaluating the effectiveness of the model in identifying important nodes. identifying important nodes Nobel Prize laureates in Physics have made profound impacts on the field and are widely recognized as the most influential group in this domain, which makes them an ideal benchmark for evaluating model performance. The APS dataset contains 140 Nobel Prize laureates in Physics. We evaluate the performance of the proposed random walk in identifying key nodes using the mean rank of benchmark nodes and AUC, comparing it with Classical Random Walk and Linear Random Walk. Lower mean rank values indicate better model performance. AUC essentially represents the probability that a randomly selected benchmark node ranks higher than a randomly selected non-benchmark node. To calculate the AUC, we control for N independent comparisons of rankings between benchmark and non-benchmark nodes, recording $N^{'}$ as the number of times the ranking of benchmark nodes exceeds that of non-benchmark nodes, and $N^{''}$ as the number of times their rankings are the same. The AUC is then defined as follows:

$$AUC = \frac{N^{'} + 0.5N^{''}}{N} \tag{6}$$

The range of AUC is between 0.5 and 1.0, with higher values indicating a stronger ability to rank benchmark nodes in higher positions. The comparison results are shown in Table 2.

It is evident that our proposed Nonlinear Random Walk outperforms both the Classical Random Walk and the Linear Random Walk in terms of both mean rank and AUC, indicating that this model can more accurately identify and evaluate scientists with high academic influence. This advantage stems from the fact that the nonlinear model, by introducing a nonlinear transition mechanism, better captures the differences in collaboration strength and heterogeneous features in academic networks, thereby enabling scientists with truly significant academic contributions to achieve higher rankings.

To validate the effectiveness of different random walk models in identifying critical nodes, we conduct node removal experiments across all three datasets. This approach provides a robust evaluation framework that does not rely on ground truth labels. The rationale is that if a model can accurately identify nodes that are crucial to the network structure, removing these top-ranked nodes should cause the network to disintegrate or lose connectivity more rapidly compared to removing randomly selected or lower-ranked nodes. In hypergraph structures, critical nodes typically serve as bridges connecting multiple communities, coordinating information flow across different groups, and maintaining the overall connectivity of the network. Therefore, the removal of such nodes would precipitate rapid network fragmentation, making node removal experiments particularly well-suited for evaluating the ability of models to identify structurally important nodes.

We ranked the stationary distributions obtained from the three random walk models in descending order, and sequentially removed different proportions of top-ranked nodes according to the rankings. When removing a node, we simultaneously deleted all hyperedges containing that node to simulate the cascading effect of node removal on the network structure. For each removal proportion ρ, we calculated three structural integrity metrics of the remaining hypergraph. We measured the relative size of the giant connected component $R(\rho)$, defined as $\frac{N_{gcc}(\rho)}{N_{remaining}(\rho)}$ for convenient cross-comparison across different removal proportions, where $N_{gcc}(\rho)$ is the number of nodes in the giant connected component of the remaining network, $N_{remaining}(\rho)$ is the total number of remaining nodes after removal, and N is the total number of nodes in the original hypergraph. This metric reflects the overall connectivity of the hypergraph. We also tracked the number of connected components $N_{cc}(\rho)$, which directly reflects the degree of network fragmentation. Additionally, we computed the average size of connected components $\bar{S}(\rho) = \frac{N_{remaining}(\rho)}{N_{cc}(\rho)}$, which reflects the average scale of network fragments.

Fig. 4 illustrates the performance of node removal experiments on the APS dataset based on node importance rankings derived from three random walk models and hyperdegree centrality (HD). Notably, the node rankings based on hyperdegree centrality are highly similar to those obtained from the CRW model, resulting in nearly overlapping performance curves in the figure. This similarity is theoretically expected, as in classical random walks on hypergraphs, a node's stationary distribution is proportional to its degree in the projected graph, which directly relates to its hyperdegree. This observation suggests that despite different computational approaches, hyperdegree centrality and CRW essentially capture similar structural properties of nodes in hypergraphs. At very small removal fractions ($\rho < 0.03$), NRW exhibits only slightly better performance than CRW across all three metrics, with both $R(\rho)$ and $\bar{S}(\rho)$ declining rapidly while $N_{cc}(\rho)$ increases sharply. In contrast, LRW performs significantly worse. As the removal fraction increases ($\rho > 0.04$), the superiority of NRW over CRW becomes increasingly evident. NRW consistently demonstrates the strongest network disruption capability. When $\rho = 0.10$, $R(\rho)$ for the NRW drops to approximately 0.03, nearly dismantling the giant component entirely, whereas CRW maintains $R(\rho)$ at around 0.08, and LRW at 0.28, showing substantially weaker disruption capability. Moreover, $N_{cc}(\rho)$ for the NRW reaches approximately 150,000, indicating that the hypergraph has largely fragmented into isolated nodes or minimal components. Furthermore, $\bar{S}(\rho)$ also reaches its lowest level, further validating its precision in

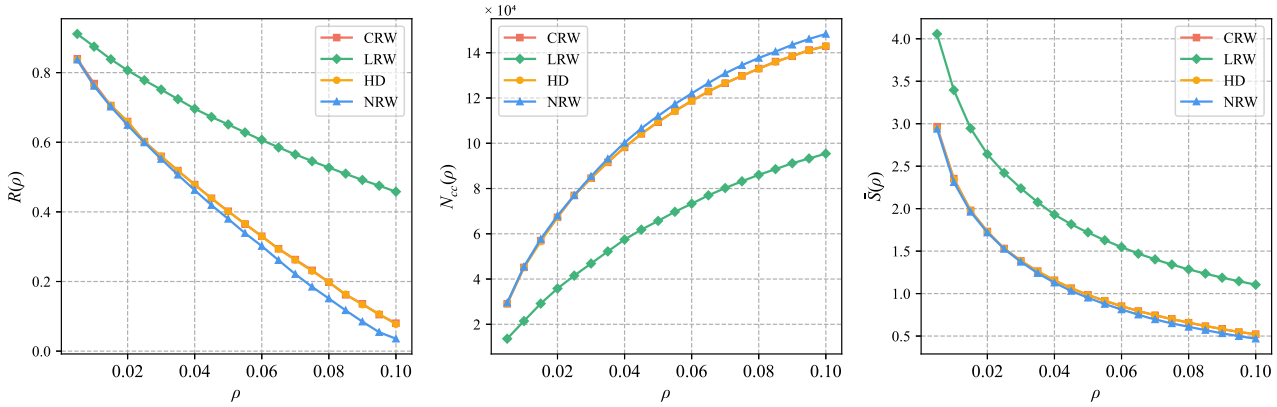

Fig. 4. Comparison of three structural integrity metrics for Hyperdegree centrality, Classical, Linear, and Nonlinear random walk models at different removal fractions. From left to right: Relative size of the giant component $R(\rho)$, number of connected components $N_{cc}(\rho)$, and average component size $\bar{S}(\rho)$. Note that for the average component size, the logarithm of the values is plotted for better visualization of the comparative effects.

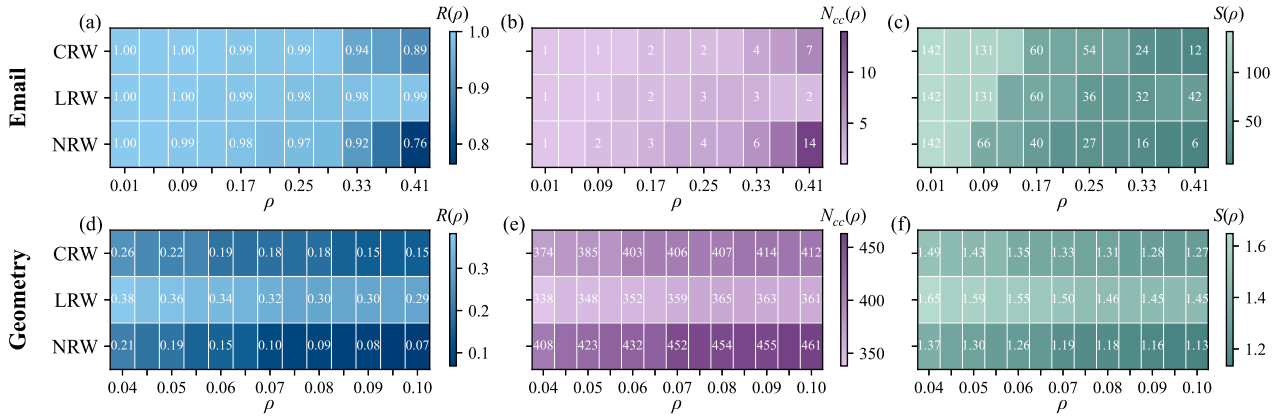

Fig. 5. Heatmaps showing the performance of node removal experiments on Email and Geometry datasets. The three structural integrity metrics R(ρ), $N_{cc}(\rho)$, and S(ρ) are evaluated for Classical, Linear, and Nonlinear random walk models across different removal fractions ρ. (a-c) Results for the Email dataset; (d-f) Results for the Geometry dataset. Numbers in cells represent metric values.

identifying critical nodes. These results demonstrate that nodes identified by the Nonlinear Random Walk are indeed critical to network robustness, as their removal triggers the most severe structural collapse.

For the Email and Geometry datasets, we employ heatmaps to visualize the results in Fig. 5. Across both datasets, the NRW consistently outperforms the CRW and LRW models across all three structural integrity metrics. For the Email dataset, the NRW achieves the most rapid decline in R(ρ), the highest network fragmentation in $N_{cc}(\rho)$, and the smallest average component sizes in S(ρ), demonstrating superior ability to identify critical nodes. The Geometry dataset exhibits extreme vulnerability to critical node removal, revealing its inherently fragile structural robustness. As shown in Fig. 5 (d)-(f), R(ρ) values drop precipitously across all models, while $N_{cc}(\rho)$ values are substantially higher, indicating that removing even small proportions of nodes causes rapid connectivity loss and highly fragmented network structure.

Across the three datasets examined, the Nonlinear Random Walk model shows consistently better performance in identifying critical nodes essential for maintaining network structural integrity. This enhanced performance stems from its ability to capture higher-order interactions within hypergraph structures, enabling the identification of nodes occupying strategically significant positions in the network. Our node removal experiments not only validate the effectiveness of the proposed importance measure but also reveal the intrinsic connection between network vulnerability and structural centrality. Specifically, high-centrality nodes identified by the Nonlinear Random Walk model correspond precisely to critical vulnerability points—when these nodes are removed, the network suffers the most severe structural damage. In contrast, the Classical Random Walk demonstrates moderate performance that deteriorates with increasing removal fractions, while the Linear Random Walk exhibits relatively limited effectiveness across all datasets. These comparative results indicate that nonlinear characteristics in higher-order interactions effectively capture structural dependencies influencing network robustness, providing new insights into vulnerability patterns of complex networks and theoretical foundations for strategies aimed at enhancing structural stability.

5. Conclusion

Considerable efforts have been devoted to investigating higher-order interactions in complex systems. Here we introduce and systematically study a Nonlinear Random Walk on hypergraphs that account for higher-order interactions. We go beyond the linear assumption inherent in traditional random walks by introducing a nonlinear mapping between transition probabilities and node hyperdegrees. Specifically, the probability of a node selecting a hyperedge is inversely proportional to a power function of its hyperdegree, where the exponent is determined by the interaction order. This design enables a more realistic characterization of dynamical behavior in systems with higher-order interactions. We prove the existence of the stationary distribution for the proposed

nonlinear random walk, thereby establishing a solid mathematical foundation for the model.

We conduct extensive numerical experiments on both synthetic and real-world networks. First, by constructing star-clique hypergraph structures, we perform a qualitative analysis of the stationary distribution and mean first hitting time obtained from our Nonlinear Random Walk model, and systematically compare them with those from the Classical Random Walk and Linear Random Walk models. The results demonstrate that the stationary distribution and mean first hitting time from our model differ significantly from those obtained by these two methods, fully revealing the fundamental impact of higher-order interactions on system dynamics. Furthermore, we apply this framework to three large-scale datasets to validate the effectiveness of the model from two perspectives. First, in the APS dataset, we compare the ranking performance of the three random walk models based on their stationary distributions using benchmark nodes. The results show that our NRW achieves the highest mean ranking for Nobel laureates, demonstrating its superior capability in identifying scientists with significant academic influence. Subsequently, we conduct node removal experiments across all three datasets. The results demonstrate that the proposed model more precisely identifies nodes crucial to network structural integrity, whereas the LRW performs poorly. These findings support the practical utility of the nonlinear random walk model and suggest its potential to guide resource allocation in network protection strategies, contributing to resilience research.

Looking ahead, this framework provides several directions for future research. On one hand, applying this model to diverse real-world networks may reveal novel phenomena driven by higher-order interactions, deepening our understanding of complex systems where group interactions are prevalent. On the other hand, the nonlinear framework provides a foundation for investigating more complex dynamical processes on hypergraphs, such as epidemic spreading, opinion dynamics, and synchronization phenomena. Furthermore, extending this approach to temporal hypergraphs and multilayer structures could yield additional insights into the interplay between network topology and dynamics.

CRediT authorship contribution statement

Meng Li: Writing – review & editing, Writing – original draft, Validation, Software, Methodology, Conceptualization; **Xin Lu:** Writing – review & editing, Validation, Supervision, Resources; **Shuiling Shi:** Software, Investigation, Data curation; **Leyang Xue:** Methodology, Investigation, Formal analysis; **Zengru Di:** Supervision, Methodology, Conceptualization.

Data availability

Data will be made available on request.

Declaration of competing interest

The authors declare that they have no known competing financial interests or personal relationships that could have appeared to influence the work reported in this paper.

Acknowledgement

This work was supported by the National Natural Science Foundation of China (72025405, 72421002, 92467302, 12575033, 72301285, 72474223), the Major Program of Xiangjiang Laboratory (24XJJCYJ01001), the Basic and Applied Research Foundation of GuangDong Province (2023A1515110176), and the Philosophy and Social Science Foundation of Guangdong Province (GD24CTS03).

Supplementary material

Supplementary material associated with this article can be found in the online version at 10.1016/j.ress.2026.112307.

References

[1] Liu Y-Y, Barabási A-L. Control principles of complex systems. Rev Mod Phys 2016;88(3):035006.
[2] Wang W-X, Lai Y-C, Grebogi C. Data based identification and prediction of nonlinear and complex dynamical systems. Phys Rep 2016;644:1–76.
[3] Tao P, Du C, Xiao Y, Zeng C. Data-driven detection of critical points of phase transitions in complex systems. Commun Phys 2023;6(1):311.
[4] Katz JS, Ronda-Pupo GA. Cooperation, scale-invariance and complex innovation systems: a generalization. Scientometrics 2019;121(2):1045–65.
[5] Xue L, Gao S, Gallos LK, Levy O, Gross B, Di Z, et al. Nucleation phenomena and extreme vulnerability of spatial k-core systems. Nat Commun 2024;15(1):5850.
[6] Ji P, Ye J, Mu Y, Lin W, Tian Y, Hens C, et al. Signal propagation in complex networks. Phys Rep 2023;1017:1–96.
[7] Shi D, Shang F, Chen B, Expert P, Lü L, Stanley HE, et al. Local dominance unveils clusters in networks. Commun Phys 2024;7(1):170.
[8] Huang Y, Wang H, Ren X-L, Lü L. Identifying key players in complex networks via network entanglement. Commun Phys 2024;7(1):19.
[9] Wang Z, Gao F, Deng Y, Ding Y, Wu J. Probabilistic disintegration for spatial network. Reliab Eng Syst Saf 2025;:111880.
[10] Boccaletti S, Latora V, Moreno Y, Chavez M, Hwang D-U. Complex networks: structure and dynamics. Phys Rep 2006;424(4–5):175–308.
[11] Zhang Z-K, Liu C, Zhan X-X, Lu X, Zhang C-X, Zhang Y-C. Dynamics of information diffusion and its applications on complex networks. Phys Rep 2016;651:1–34.
[12] Battiston F, Cencetti G, Iacopini I, Latora V, Lucas M, Patania A, et al. Networks beyond pairwise interactions: structure and dynamics. Phys Rep 2020;874:1–92.
[13] Battiston F, Amico E, Barrat A, Bianconi G, Ferraz de Arruda G, Franceschiello B, et al. The physics of higher-order interactions in complex systems. Nat Phys 2021;17(10):1093–8.
[14] Tamura M, Spellman TJ, Rosen AM, Gogos JA, Gordon JA. Hippocampal-prefrontal theta-gamma coupling during performance of a spatial working memory task. Nat Commun 2017;8(1):2182.
[15] Iacopini I, Petri G, Barrat A, Latora V. Simplicial models of social contagion. Nat Commun 2019;10(1):2485.
[16] Rao S, Ahmad K, Ramachandran S. Cooperative binding between distant transcription factors is a hallmark of active enhancers. Mol Cell 2021;81(8):1651–65.
[17] Beyza J, Yusta JM. The effects of the high penetration of renewable energies on the reliability and vulnerability of interconnected electric power systems. Reliab Eng Syst Saf 2021;215:107881.
[18] Zhao T, Tu H, Jin R, Xia Y, Wang F. Improving resilience of cyber–physical power systems against cyber attacks through strategic energy storage deployment. Reliab Eng Syst Saf 2024;252:110438.
[19] Jia C-X, Liu R-R. Higher-order interdependencies and connectivity: a dual-layer hypergraph model for cascading failures. Reliab Eng Syst Saf 2025;:111850.
[20] Qian C, Zhao D, Zhong M, Peng H, Wang W. Modeling and analysis of cascading failures in multilayer higher-order networks. Reliab Eng Syst Saf 2025;253:110497.
[21] Li J, Yuan X, Fu Y, Li J, Tan W, Lu X. Representing significant dependencies with variable orders in networks. Chaos Soliton Fractal 2025;201:117405. https://doi.org/10.1016/j.chaos.2025.117405
[22] Li J, Lu X. Measuring the significance of higher-order dependency in networks. New J Phys 2024;26(3):033032.
[23] Bick C, Gross E, Harrington HA, Schaub MT. What are higher-order networks? SIAM Rev 2023;65(3):686–731.
[24] Gao Z, Ghosh D, Harrington HA, Restrepo JG, Taylor D. Dynamics on networks with higher-order interactions. Chaos: Interdiscip J Nonlinear Sci 2023;33(4).
[25] Landry NW, Restrepo JG. The effect of heterogeneity on hypergraph contagion models. Chaos: Interdisciplinary J Nonlinear Sci 2020;30(10).
[26] Millán AP, Torres JJ, Bianconi G. Explosive higher-order kuramoto dynamics on simplicial complexes. Phys Rev Lett 2020;124(21):218301.
[27] Gambuzza LV, Di Patti F, Gallo L, Lepri S, Romance M, Criado R, et al. Stability of synchronization in simplicial complexes. Nat Commun 2021;12(1):1255.
[28] St-Onge G, Sun H, Allard A, Hébert-Dufresne L, Bianconi G. Universal nonlinear infection kernel from heterogeneous exposure on higher-order networks. Phys Rev Lett 2021;127(15):158301.
[29] Lucas M, Cencetti G, Battiston F. Multiorder laplacian for synchronization in higher-order networks. Phys Rev Res 2020;2(3):033410.
[30] Boccaletti S, De Lellis P, Del Genio CI, Alfaro-Bittner K, Criado R, Jalan S, et al. The structure and dynamics of networks with higher order interactions. Phys Rep 2023;1018:1–64.
[31] Bodó Á, Katona GY, Simon PL. Sis epidemic propagation on hypergraphs. Bull Math Biol 2016;78:713–35.
[32] Chowdhary S, Kumar A, Cencetti G, Iacopini I, Battiston F. Simplicial contagion in temporal higher-order networks. J Phys: Complex 2021;2(3):035019.
[33] de Arruda GF, Petri G, Moreno Y. Social contagion models on hypergraphs. Phys Rev Res 2020;2(2):023032.
[34] Ferraz de Arruda G, Petri G, Rodriguez PM, Moreno Y. Multistability, intermittency, and hybrid transitions in social contagion models on hypergraphs. Nat Commun 2023;14(1):1375.

[35] Neuhäuser L, Mellor A, Lambiotte R. Multibody interactions and nonlinear consensus dynamics on networked systems. Phys Rev E 2020;101(3):032310.
[36] Schawe H, Hernández L. Higher order interactions destroy phase transitions in deffuant opinion dynamics model. Commun Phys 2022;5(1):32.
[37] Mulas R, Kuehn C, Jost J. Coupled dynamics on hypergraphs: master stability of steady states and synchronization. Phys Rev E 2020;101(6):062313.
[38] Petit J, Lambiotte R, Carletti T. Classes of random walks on temporal networks with competing timescales. Appl Netw Sci 2019;4(1):72.
[39] Skardal PS, Adhikari S. Dynamics of nonlinear random walks on complex networks. J Nonlinear Sci 2019;29(4):1419–44.
[40] Schaub MT, Benson AR, Horn P, Lippner G, Jadbabaie A. Random walks on simplicial complexes and the normalized hodge 1-laplacian. SIAM Rev 2020;62(2):353–91.
[41] Mukherjee S, Steenbergen J. Random walks on simplicial complexes and harmonics. Random Struct Algorithm 2016;49(2):379–405.
[42] Zhou D, Huang J, Schölkopf B. Learning with hypergraphs: clustering, classification, and embedding. Adv Neural Inf Process Syst 2006;19.
[43] Carletti T, Battiston F, Cencetti G, Fanelli D. Random walks on hypergraphs. Phys Rev E 2020;101(2):022308.
[44] Helali A, Löwe M. Hitting times, commute times, and cover times for random walks on random hypergraphs. Stat Probab Lett 2019;154:108535.
[45] Chitra U, Raphael B. Random walks on hypergraphs with edge-dependent vertex weights. In: International conference on machine learning. PMLR; 2019, p. 1172–81.
[46] Zeng Y, Huang Y, Ren X-L, Lü L. Identifying vital nodes through augmented random walks on higher-order networks. Inf Sci (Ny) 2024;679:121067.